



Solvent Media on Nonlinear Optical Properties of Triarylmethane Dye via Facile Z-Scan Method

N. Srinivasan Arunsankar¹ · A. Prabakaran² · P. Saravanan³ · M. Vimalan³ · S. Jeyaram⁴

Received: 23 October 2023 / Accepted: 26 November 2023

© The Author(s), under exclusive licence to Springer Science+Business Media, LLC, part of Springer Nature 2023

Abstract

Solvent environment on third-order nonlinear optical (TNLO) features of triarylmethane dye namely, basic blue 7 in different solvents is reported herein using 650 nm diode laser with continuous wave mode. The basic blue 7 dye is dissolved in different solvent media including ethanol, methanol, dimethyl formamide (DMF) and dimethyl sulfoxide (DMSO). The influence of solvent characteristics such as solvent polarizability and dipole moment on solute molecule is discussed. TNLO characteristics such as nonlinear optical index of refraction, nonlinear optical coefficient of absorption, real and imaginary components of the TNLO susceptibility are measured to be the order of 10^{-7} cm²/W, 10^{-3} cm/W, 10^{-6} esu and 10^{-7} esu, respectively. The dye exhibits large TNLO susceptibility by dissolving in DMSO. The TNLO susceptibility of basic blue 7 dye is measured to be the order of 10^{-6} esu. The overall results revealed that the basic blue 7 dye is suitable material for optoelectronics applications.

Keywords TNLO · Nonlinear optical properties · Z-scan · Basic blue 7 dye · Solvent characteristics

Introduction

Nonlinear optics is the thrust area in physics which is widely applied in optical switching and limiting, optical data storage, optical computing, optical communication, 3D image photography, three photon microscopy, etc. [1–5]. Nonlinear optical (NLO) materials are the key role for above mentioned applications. Verity of materials including organic dyes [6–10], single crystal [11], semiconducting materials [12], nanomaterials [13], graphene [14], polymer nanocomposites [15], natural pigments [16–18], etc., are used recently for NLO study. Among these materials, organic dyes are always

increasing the interest of the researchers due to high TNLO susceptibility, large molecular polarizability, high stability, structural flexibility, etc. [19, 20]. Variety of dyes with corresponding families such as azo [21], triphenylmethane [22], triarylmethane [23], indigo [24], anthraquinone [25], thiazine [26], cyanine [27], styryl [28] and xanthene [29] are involved in TNLO study. Basic blue 7 dye is a triarylmethane family which is predominantly used in textile dyeing, including wool, silk, cotton, and leather.

Various experimental techniques are used to quantify the TONLO features of the compounds such as degenerate four-wave and three-wave mixing, ellipse rotation, beam distortion, Z-scan technique, etc. [30–34]. Among the available experimental techniques, Z-scan is the most sensitive and simple tool to calculate the TONLO characteristics of the materials [35]. This technique has wide advantages including easy experimental procedure, sign and magnitude of the NLO index of refraction and NLO coefficient of absorption is simultaneously measured from closed and open aperture techniques, simple calculation, real and imaginary features of the sample is simultaneously measured from the experiments, etc.

NLO features of solute molecules changes with respect to molecular surrounding environment [36]. The TNLO properties of organic molecules increases with decrease

✉ S. Jeyaram
jeyaram.msc@gmail.com

¹ Department of Physics, Sri Sairam Engineering College, West Tambaram, Chennai 600044, Tamilnadu, India

² Department of Physics, Veltech Rangarajan Dr. Sagunthala R&D Institute of Science and Technology, Avadi, Chennai 600062, Tamilnadu, India

³ Department of Physics, Saveetha School of Engineering, Saveetha Institute of Medical and Technical Sciences, Chennai 602105, Tamilnadu, India

⁴ Department of Physics, Takshashila University, Ongur (PO), Tindivanam, Villupuram 604305, Tamilnadu, India

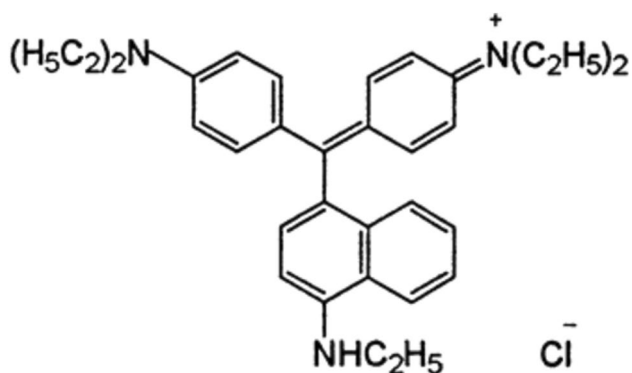


Fig. 1 Molecular structure of basic blue 7 dye

in energy gap between highest occupied molecular orbit (HOMO) and lowest unoccupied molecular orbit (LUMO). The HOMO–LUMO energy gap is decreased by two ways; one is structural modification and another one is solute–solvent interaction. The interaction between solvent and solute molecule can change the physical, chemical and biological behaviors of the sample and are divided into non-specific and specific interaction. Specific interactions include hydrogen bond and intermolecular charge transfer, whereas non-specific interactions comprises of dielectric enrichment [37]. The solvent effect on the solute molecules is calculated by solvatochromism and solvent polarity index [37].

This paper reports the TNLO features of basic blue 7 dye in different solvents such as ethanol, methanol, acetone, 1-propanol, DMF and DMSO.

Materials and Methods

All the chemicals and basic blue 7 dye are purchased from Sigma Aldrich and used as such. The dye is dissolved into ethanol, methanol, DMF and DMSO with 0.01 mM concentrations. The molecular structure of the dye is shown in Fig. 1. Table 1 represents the spectral properties of the used solvents and linear absorption coefficient of basic blue 7 dye.

Table 1 Linear optical properties of basic blue 7 dye and spectral parameters of polar solvents

Solvent	Linear refractive index (n_0)	Dielectric constant (ϵ)	Hydrogen bond donor (α)	Hydrogen bond acceptor (β)	Polarizability (π^*)	Linear absorption coefficient (α_0/cm)
Methanol	1.329	32.7	0.98	0.66	0.60	2.09
Ethanol	1.361	24.50	0.86	0.75	0.52	5.50
DMF	1.430	38.00	0.00	0.69	0.88	5.79
DMSO	1.479	46.68	0.00	0.76	1.00	5.09

Z-Scan Technique

The Z-scan experimental method is shown in Fig. 2. A semiconductor diode laser with a CW output power of 5 mW operating at a wavelength of 650 nm is used for the studies. A convex lens with 50 mm focal length is placed before the cuvette. A 1 mm thick cuvette is filled with the basic blue 7 dye in various solvents is placed on the micrometer stage and translate from -Z to +Z positions. The closed aperture and open aperture techniques are used to measure the n_2 and β of basic blue 7 dye. To measure the beam transmittance, a power meter is positioned at far from the source. The condition for thin sample is validated because the measured Rayleigh length is greater than sample length ($Z_R > L$).

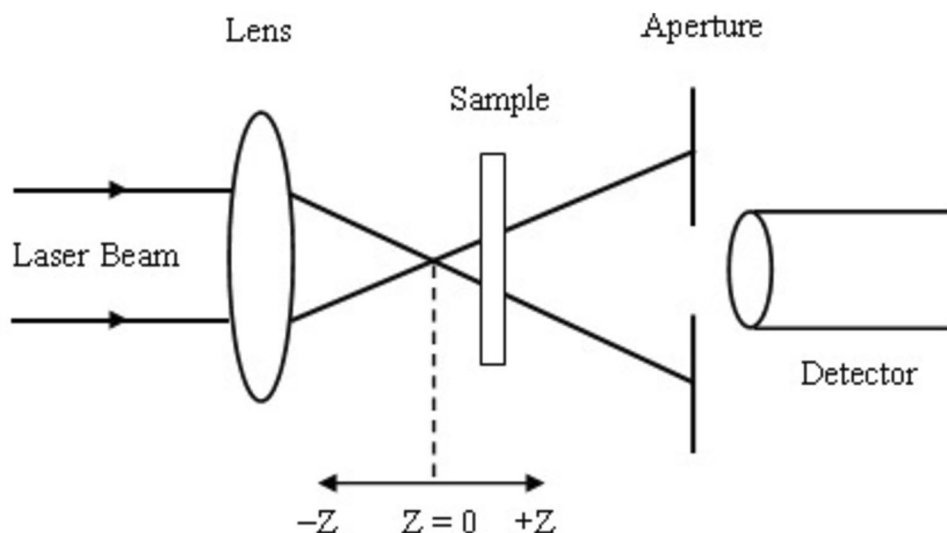
Results and Discussions

UV-Visible Absorption Study

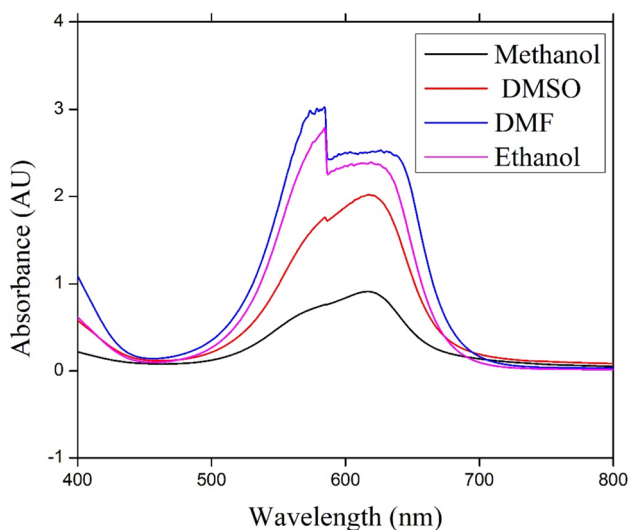
Figure 3 shows the UV-Visible absorption spectrum of basic blue 7 dye. The absorbance of basic blue 7 dye in ethanol, methanol, DMF and DMSO is 612 nm, 619 nm, 605 nm 617 nm, respectively. Furthermore, the maximum absorbance of basic blue 7 dye is observed when the dye sample is dissolved in DMF. The absorption maximum of the dye sample is shifted towards the red region of the spectrum by increasing the solvent polarizability. This may be due to the result of π - π^* transition where the excited states is more polarized than the ground state [38]. This is known as red shift or bathochromic shift.

TNLO Study

The open aperture (OA) and closed aperture (CA) Z-scan techniques are used to calculate the TNLO susceptibility ($\chi^{(3)}$) of the sample. In the CA approach, an aperture is positioned in front of the detector with an appropriate opening so that only the center portion of the Gaussian beam enters into the detector. In OA method, a converging lens is used to

Fig. 2 Experimental setup for the Z-scan measurement

collect the beam transmittance, which is positioned in front of the detector. Closed and open aperture techniques are used to calculate the sample's nonlinear index of refraction and nonlinear coefficient of absorption, which are directly related to the real component and imaginary part of $\chi^{(3)}$ respectively. Figure 4(a–d) illustrates the open aperture result of basic blue 7 dye in ethanol, methanol, DMF and DMSO at 0.01 mM concentration. In Fig. 4(a–d), the nonlinear absorption (NLA) curve of basic blue 7 dye shows both negative and positive nonlinear absorption due to saturable absorption (SA) and reverse saturable absorption (RSA) features of the dye sample. The transmittance curve of basic blue 7 dye dissolved in DMF and DMSO shows RSA character, while the sample displays SA features in ethanol and methanol. SA arises from high light intensities at the focus and therefore the photon

**Fig. 3** UV-Visible absorption spectrum of basic blue 7 dye

absorption significantly increasing before attaining to the ground state. Conversely, basic blue 7 dye is dissolved in DMF and DMSO displays RSA, due to strong interaction between the light intensity and the dye sample at the focus. The excited state absorption cross-section is larger than ground state is the consequence of RSA. Furthermore, the five level model gives the information about the nonlinear absorption mechanism of organic sample [19]. This model consists of various energy levels which contain singlet and triplet states with corresponding vibrational energy levels as shown in Fig. 5. A process that transforms a singlet ground state to excited state simultaneously by absorbing two photons of the same or different energies is known as two-photon absorption. Saturable absorption is the process in which transition from singlet state to triplet state through intersystem crossing (ISC). Transition from first singlet state to excited singlet state or first triplet state to excited triplet state is called excited-state absorption (ESA) or RSA.

The RSA is the predominant NLA mechanism in organic dyes, and it may be improved if the electrons from S_1 were moved to T_1 via an ISC from where T_2 would take place. Due to absorption of CW laser irradiation at a wavelength of 650 nm, the ESA may also contribute to the NLA process [19]. As a result, the reported NLA of basic blue 7 dye in DMF and DMSO is ESA assisted RSA. The nonlinear absorption transmittance in the open aperture approach is provided by,

$$T(z, s = 1) = \sum_{m=0}^{\infty} \frac{[-q_o(z)]^m}{[m + 1]^{\frac{3}{2}}}, \text{ for } |q_o(0)| < 1 \quad (1)$$

where

$$q_o = \frac{\beta I_o L_{eff}}{\left(1 + z^2/z_0^2\right)} \quad (2)$$

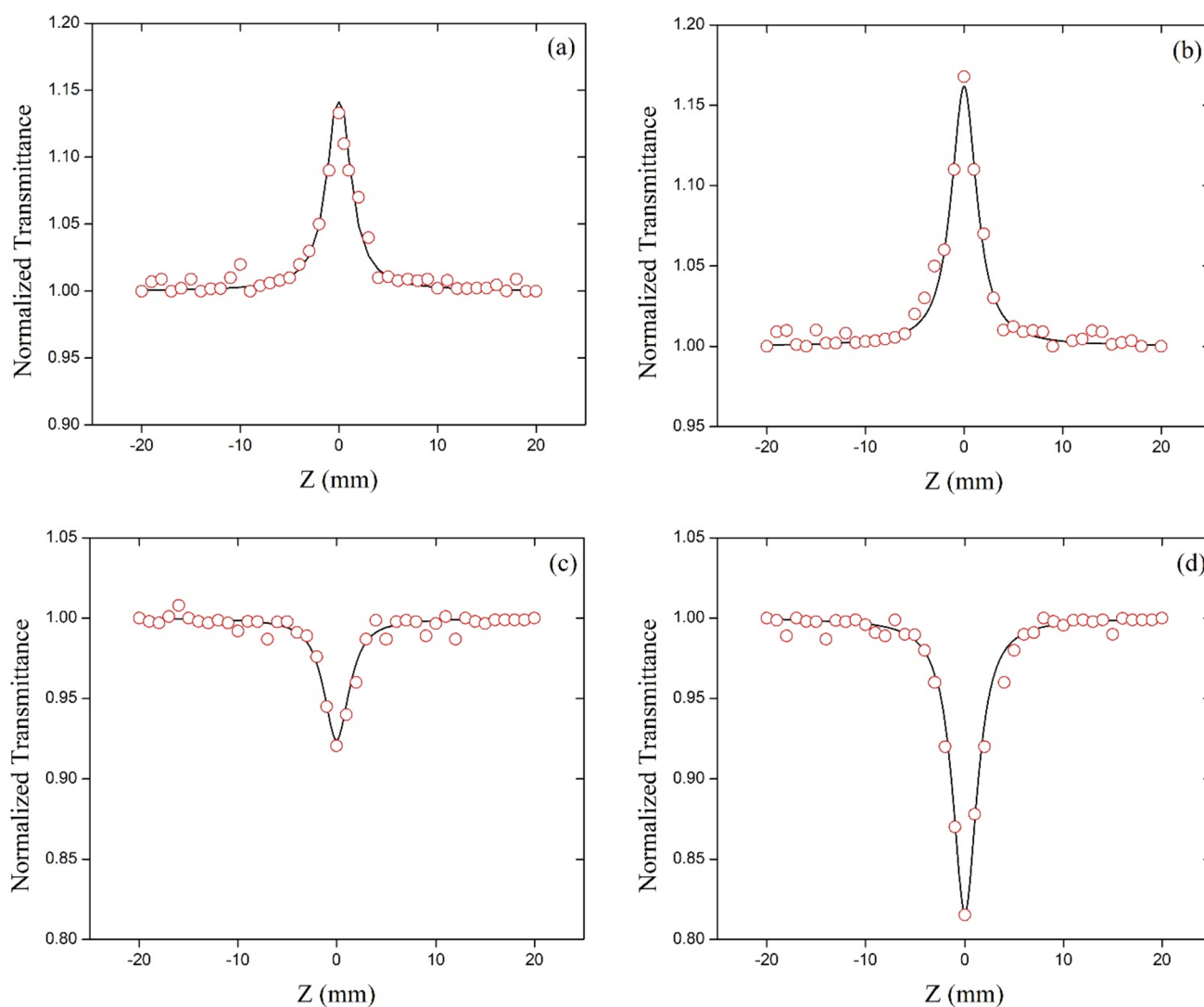


Fig. 4 Open aperture Z-scan results of basic blue 7 dye in **a** Ethanol **b** Methanol **c** DMF **d** DMSO

where L_{eff} = effective length of the sample and Z_0 = sample diffraction length. The nonlinear absorption coefficient (β) is given by,

$$\beta = \frac{2\sqrt{2}\Delta T}{I_0 L_{\text{eff}}} \left(\frac{\text{cm}}{\text{W}} \right) \quad (3)$$

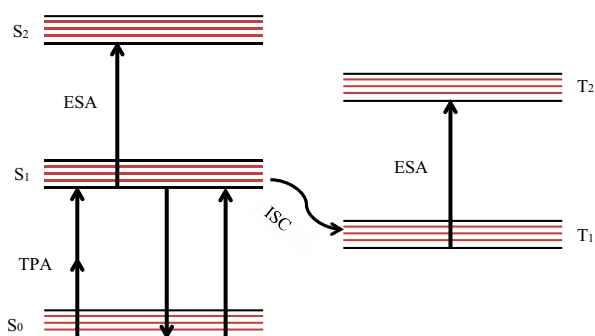


Fig. 5 Five-level energy diagram

The sign and magnitude of nonlinear refractive index are determined using the CA method. The nonlinear refraction measured from closed technique includes the influence of NLR and NLA [35]. Therefore, the pure portion of NLR is obtained by dividing the relevant open aperture data from the closed aperture data. Figure 6(a–d) shows the pure nonlinear refraction curve of basic blue 7 dye in ethanol, methanol, DMF and DMSO. The curve exhibits pre focal peak followed by post focal valley transmittance in all the solvents is the outcome of self-defocusing. Self-defocusing is arises from thermal nonlinearity which arises from the continuous absorption of used light source. Thermal lensing results from a change in the sample's

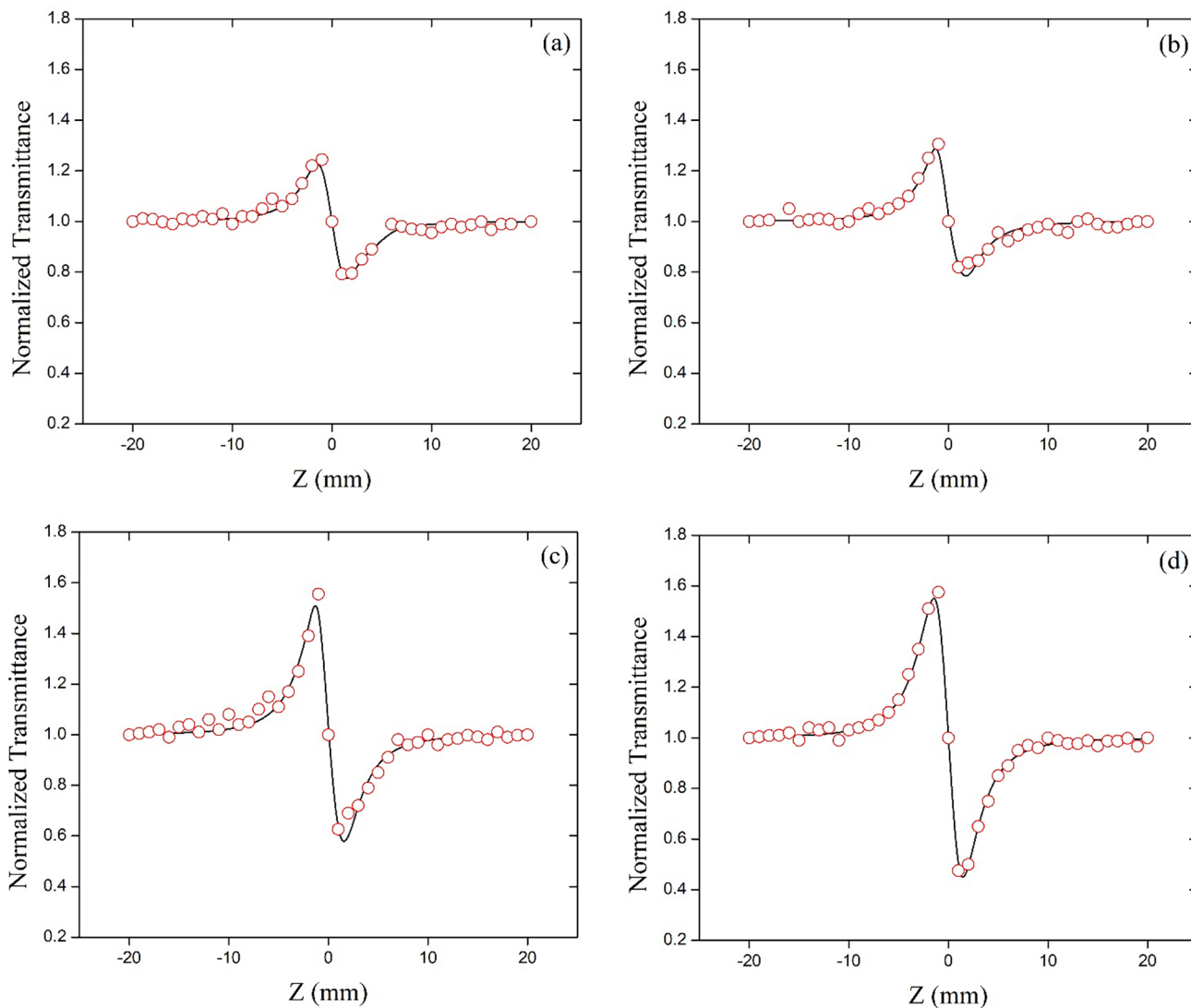


Fig. 6 Pure nonlinear refraction results of basic blue 7 dye in a Ethanol b Methanol c DMF d DMSO

internal temperature brought on by the continuous wave (CW) laser irradiation. The sample acts as a defocusing lens when its temperature rises and its index of refraction turns negative. The origin of nonlinear refraction in materials may be electronic, molecular, electrostatic or thermal nonlinearity [35]. In organic samples thermal nonlinearity is the leading mechanism which is confirmed by peak-valley separation. The peak-valley separation is 1.7 times the Rayleigh length is the clear indication of thermal nonlinearity [35]. The normalized transmittance of the dye sample is given by,

$$T(z) = 1 - \Delta\varnothing_o \frac{4X}{(X^2 + 1)(X^2 + 9)} \tag{4}$$

where $X = Z/Z_0$.

The nonlinear index of refraction (n_2) is calculated by using the relation

$$n_2 = \frac{\Delta\varnothing_0 \lambda}{2\pi I_0 L_{eff}} \left(\frac{m^2}{W} \right) \tag{5}$$

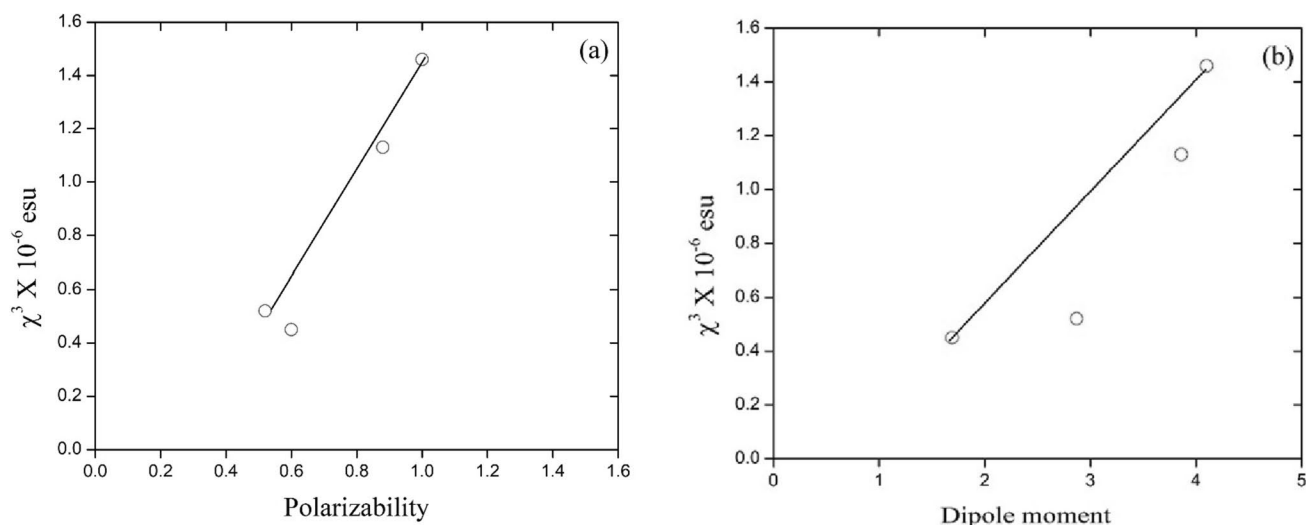
where $\Delta\varnothing_0$ = On-axis phase shift, λ = Wavelength of the light source and I_0 = Intensity of the light beam at the focus.

The measured value of nonlinear refractive index of basic blue 7 dye in ethanol, methanol, DMF and DMSO solvents is tabulated in Table 2. The real and imaginary components of $\chi^{(3)}$ is given by,

$$Re[\chi^{(3)}] (esu) = \frac{\epsilon_0 c^2 n_0^2}{10^4 \pi} n_2 \left(\frac{cm^2}{W} \right) \tag{6}$$

Table 2 TONLO characteristics of basic blue 7 dye

Solvent	$n_2 \times 10^{-7}$ (cm^2/W)	$\beta \times 10^{-3}$ (cm/W)	$\text{Re}(\chi^3) \times 10^{-6}$ (esu)	$\text{Im}(\chi^3) \times 10^{-7}$ (esu)	$\chi^{(3)} \times 10^{-6}$ (esu)
Methanol	-1.39	-4.69	-0.45	-0.59	0.45
Ethanol	-2.79	-3.37	-0.51	-0.37	0.52
DMF	-3.02	2.64	-1.13	0.51	1.13
DMSO	-3.62	5.94	-1.45	1.23	1.46

**Fig. 7** TONLO susceptibility (χ^3) of basic blue 7 dye as a function of **a** polarizability and **b** dipole moment of the solvents

$$\text{Im}[\chi^{(3)}](\text{esu}) = \frac{\epsilon_0 c^2 n_0^2 \lambda}{10^2 4\pi^2} \beta \left(\frac{\text{cm}}{\text{W}} \right) \quad (7)$$

where c = velocity of light in vacuum and ϵ_0 = vacuum permittivity. The TONLO susceptibility of basic blue 7 dye is given by,

$$\chi^{(3)} = \sqrt{(\text{Re}(\chi^3))^2 + (\text{Im}(\chi^3))^2}(\text{esu}) \quad (8)$$

The calculated value of TONLO susceptibility $\chi^{(3)}$ of basic blue 7 dye is presented in Table 2. It is noted from Table 2 that, the dye sample exhibits large nonlinear optical susceptibility in DMSO than other polar solvents.

The solvent effect on the solute molecules was determined by solvent polarity scale or solvatochromism. The solvent environment plays a major role between solute and solvent interaction and it influences the TONLO characteristics of the materials [36]. Solvent parameters such as solvent hydrogen bond donor, solvent hydrogen bond acceptor, dipole moment and polarizability are the major spectral factors that affecting the TONLO properties of the sample. Figure 7(a) & (b) shows the TONLO susceptibility of basic blue 7 dye as a function of polarizability and dipole moment of the polar solvents. It is noticed in Fig. 7(a) & (b) that the

TONLO susceptibility of basic blue 7 dye increases with increase in solvent polarizability and dipole moment. Furthermore, the nonlinear absorption coefficient of basic blue 7 dye switchover from saturable absorption to reverse saturable absorption due to increase in solvent polarizability and dipole moment.

Conclusion

In conclusion, the TONLO features of basic blue 7 dye in ethanol, methanol, DMF and DMSO at 0.01 mM concentration was studied using single beam Z-scan technique. The UV-Vis absorption spectrum revealed that the dye sample possesses positive solvatochromism by increasing the polarity of the solvent. TONLO features of the dye sample was studied using 5 mW power laser working at 650 nm wavelength. The open aperture curve of the dye sample in different solvents exhibits both SA and RSA properties and closed aperture transmittance revealed the character of self-defocusing. The self-defocusing effect is the result of thermal nonlinearity. The order of TONLO susceptibility $\chi^{(3)}$ of basic blue 7 dye in polar solvents was found to be 10^{-6} esu. The basic blue 7 dye exhibit large optical nonlinearity when

it dissolved in high polar solvent such as DMF and DMSO. The results suggest that the dye sample studied here is a potential material for future NLO applications.

Author Contributions Conceptualization—Srinivasan Arunsankar N & Prabakaran A Methodology—Vimalan M & Srinivasan Arunsankar N & Validation—Prabakaran A Vimalan M, Writing-review and editing—Saravanan P & Jeyaram S and Supervision—Jeyaram S.

Funding None.

Availability of Data and Materials All the data available with the authors.

Declarations

Ethics Approval The submitted work should be original and should not have been published elsewhere in any form or language.

Consent to Participate Yes.

Consent for Publication Yes granted.

Informed Consent Not applicable.

Research Involving Human Participants and/or Animals Research involving human participants.

Competing Interests The authors declare no competing interests.

References

- Sreenath MC, Hubert Joe I, Rastogi VK (2018) Third-order optical nonlinearities of 1,4-diaminoanthraquinone for optical limiting applications. *Opt Laser Technol* 108:218–234. <https://doi.org/10.1016/j.optlastec.2018.06.056>
- You JW, Bongu SR, Bao A, Panoiu NC (2019) Nonlinear optical properties and applications of 2D materials: Theoretical and experimental aspects. *J Nanophotonics* 8:63–97. <https://doi.org/10.1515/nanoph-2018-0106>
- Sangeetha K, Thamotharan S (2018) Thermally induced self-phase modulation and optical limiting applications of L-arginine hydrochloride (LAHCL) solutions. *Optik* 164:519–526. <https://doi.org/10.1016/j.ijleo.2018.03.029>
- Manjunatha KB, Rajarao R, Umesh G, Bhat BR, Poornesh P (2017) Optical nonlinearity, limiting and switching characteristics of novel ruthenium metal-organic complex. *Opt Mater* 72:513–517. <https://doi.org/10.1016/j.optmat.2017.06.051>
- Xu J, Semin S, Niedzialek D, Kouwer PHJ, Fron E, Coutino E, Savoini M, Li Y, Hofkens J, Uji-I H, Beljonne D, Rasing T, Rowsan AE (2013) Self-assembled organic microfibers for nonlinear optics. *Adv Mater* 25:2084–2089. <https://doi.org/10.1002/adma.201204237>
- Sadigh MK, Zakerhamidi MS (2018) Media polarity and concentration roles on the third-order nonlinear behaviors of thiazine dyes. *Opt Laser Technol* 100:216–224. <https://doi.org/10.1016/j.optlastec.2017.10.007>
- Motiei H, Jafari A, Naderali R (2017) Third-order nonlinear optical properties of organic azo dyes by using strength of nonlinearity parameter and Z-scan technique. *Opt Laser Technol* 88:68–74. <https://doi.org/10.1016/j.optlastec.2016.09.011>
- Pathrose B, Nampoory VPN, Radhakrishnan P, Mujeeb A (2016) Investigation on the third order nonlinear optical properties of Basic Fuchsin dye using Z scan technique. *Optik* 127:7717–7725. <https://doi.org/10.1016/j.ijleo.2016.05.136>
- Choubey RK, Medhekar S, Kumar R, Mukherjee S, Kumar S (2014) Study of optical properties of organic dye by Z-scan technique using He-Ne laser. *J Mater Sci Mater Elect* 25:1410–1415. <https://doi.org/10.1007/s10854-014-1743-3>
- Sadigh MK, Zakerhamidi MS, Rezaei B, Milachian K (2017) Environment effects on the nonlinear absorption properties of Methylene blue under different power of excitation beam. *J Mol Liq* 229:548–554. <https://doi.org/10.1016/j.molliq.2016.12.108>
- Parol V, Prabhu AN, Taher MA, Naraharisetty SRG, Lokanath NK, Upadhavava V (2020) A third-order nonlinear optical single crystal of 3,4-dimethoxy-substituted chalcone derivative with high laser damage threshold value: a potential material for optical power limiting. *J Mater Sci Mater Elect* 31:9133–9150. <https://doi.org/10.1007/s10854-020-03443-2>
- Saeed A, Razvi MA, Salah N (2021) Third-order nonlinear optical properties of the small-molecular organic semiconductor tris (8-Hydroxyquinoline) aluminum by CW Z-scan technique. *Results Phys* 24:104162. <https://doi.org/10.1016/j.rinp.2021.104162>
- Shokoufi N, Hajibaba SN (2019) The third-order nonlinear optical properties of gold nanoparticles-methylene blue conjugation. *Opt Laser Technol* 112:198–206. <https://doi.org/10.1016/j.optlastec.2018.09.058>
- Liu G, Dai S, Zhu B, Li P, Wu Z, Gu Y (2019) Third-order nonlinear optical properties of MoSe₂/graphene composite materials. *Opt Laser Technol* 120:105746. <https://doi.org/10.1016/j.optlastec.2019.105746>
- Prakash J, Jeyaram S (2022) Synthesis, characterization, morphological, linear and nonlinear optical properties of silicon carbide doped PVA nanocomposites. *SILICON* 14:11163–11170. <https://doi.org/10.1007/s12633-022-01852-y>
- Jeyaram S (2022) Natural pigments of aloe vera: A third-order NLO materials. *Braz J Phys* 52:24. <https://doi.org/10.1007/s13538-021-01031-1>
- Zongo S, Kerasidou AP, Sone BT, Diallo A, Mthunzi P, Iliopoulos K, Nkosi M, Maaza M, Sahraoui B (2015) Nonlinear optical properties of poly(methyl methacrylate) thin films doped with Bixa Orellana dye. *Appl Sur Sci* 340:72–77. <https://doi.org/10.1016/j.apsusc.2015.02.1610>
- Jeyaram S, Jeancy Rany D (2023) Extraction of natural pigment from ocimum tenuiflorum using different polar solvents and their nonlinear optical characteristics. *J Fluoresc* 33:287–295. <https://doi.org/10.1007/s10895-022-03061-7>
- Jeyaram S (2022) Nonlinear optical responses in organic dye by Z-scan method. *J Opt* 51:666–671. <https://doi.org/10.1007/s12596-022-00834-y>
- Pramodini S, Poornesh S (2014) Effect of conjugation length on nonlinear optical properties of anthraquinone dyes investigated using He-Ne laser operating in CW mode. *Opt Laser Technol* 62:12–19. <https://doi.org/10.1016/j.optlastec.2014.02.003>
- Anusha B, Jeyaram S (2023) Solvatochromism effect on third-order NLO properties of Azo dye. *J Opt*. <https://doi.org/10.1007/s12596-023-01217-7>
- Madahana Sundari R, Palanisamay PK (2006) Optical nonlinearity of a triphenylmethane dye as studied by Z-scan and self-diffraction techniques. *Mod Phys Lett B* 20:887–897. <https://doi.org/10.1142/S0217984906010780>
- Vinitha G, Ranalingam A (2008) Single-beam Z-scan measurement of the third-order optical nonlinearities of triarylmethane dyes. *Laser Phys* 18:1176–1182. <https://doi.org/10.1134/S1054660X08100113>

24. Pramodini S, Poornesh P (2014) Third-order nonlinear optical response of indigo carmine under 633 nm excitation for nonlinear optical applications. *Opt Laser Technol* 63:114–119. <https://doi.org/10.1016/j.optlastec.2014.04.007>
25. Jeyaram S, Naseer J, Punitha S (2021) Effect of solvent on third-order nonlinear optical behavior of reactive blue 19 dye. *J Fluoresc* 31:1895–1906. <https://doi.org/10.1007/s10895-021-02808-y>
26. Qusay Mohammed Ali (2006) Palanisamy PK, Z-scan determination of the third-order nonlinearity of organic dye Nile blue chloride. *Mod Phys Lett B* 20:623–632. <https://doi.org/10.1142/S0217984906010779>
27. Han P, Wang D, Gao H, Zhang J, Xing Y, Yang Z, Cao H, He W (2018) Third-order nonlinear optical properties of cyanine dyes with click chemistry modification. *Dyes Pigm* 149:8–15. <https://doi.org/10.1016/j.dyepig.2017.09.052>
28. Shettigar S, Umesh G, Poornesh P, Manjunatha KB, Asiri AM (2009) The third-order nonlinear optical properties of novel styryl dyes. *Dyes Pigm* 83:207–210. <https://doi.org/10.1016/j.dyepig.2009.04.009>
29. Ganeev RA, Boltaev GS, Zvyagin AI, Smirnov MS, Ovchinnikov OV (2018) Nonlinear absorption of some thiazine, xanthene, and carbocyanine dyes. *Optik* 157:113–124. <https://doi.org/10.1016/j.ijleo.2017.11.083>
30. Maker PD, Terhune RW, Savage CM (1964) Intensity-dependent changes in the refractive index of liquids. *Phys Rev Lett* 12:507–509. <https://doi.org/10.1103/PhysRevLett.12.507>
31. Veduta AP, Kirsanov BP (1968) Variation of the refractive index of liquids and glasses in a high intensity field of a ruby laser. *J Exp Theor Phys* 27:736–738
32. Buchalter B, Meredith GR (1982) Third-order optical susceptibility of glasses determined by third harmonic generation. *Appl Opt* 21:3221–3224. <https://doi.org/10.1364/AO.21.003221>
33. Adair R, Chase LL, Payne SA (1987) Nonlinear refractive-index measurements of glasses using three-wave frequency mixing. *J Opt Soc Am B* 4:875–881. <https://doi.org/10.1364/JOSAB.4.000875>
34. Wu CK (1980) Measurement of third-order susceptibility by using degenerate four-wave mixing. *Chin J Phys* 29:508–510. <https://doi.org/10.7498/aps.29.508>
35. Sheik-Bahae M, Said AA, Wei T, Hagan DJ, Van Stryland EW (1990) Sensitive measurement of optical nonlinearities using a single beam. *IEEE J Quant. Elect QE* 26:760–769. <https://doi.org/10.1109/3.53394>
36. Jeyaram S (2021) Study of third-order nonlinear optical properties of basic violet 3 dye in polar protic and aprotic solvents. *J Fluoresc* 31:1637–1644. <https://doi.org/10.1007/s10895-021-02796-z>
37. Jeyaram S (2023) Nonlinear absorption features of acid blue 129 dye in polar solvents: Role of solvents on solute molecule. *J Fluoresc*. <https://doi.org/10.1007/s10895-023-03277-1>
38. Edwards AA, Alexander BD (2017) UV-visible absorption spectroscopy, organic applications, encyclopedia of spectroscopy and spectrometry, 3rd edition, 511–519

Publisher's Note Springer Nature remains neutral with regard to jurisdictional claims in published maps and institutional affiliations.

Springer Nature or its licensor (e.g. a society or other partner) holds exclusive rights to this article under a publishing agreement with the author(s) or other rightsholder(s); author self-archiving of the accepted manuscript version of this article is solely governed by the terms of such publishing agreement and applicable law.